PAPER

An azothiazole probe as a multianalyte colorimetric chemosensor for urea and biologically significant amines†

Sapna Singh, Archana Velloth, Rishi Ram Mahato, Surbhi Grewal, Subhabrata Maiti [ID] * and Sugumar Venkataramani [ID] *

We report an azothiazole-based probe as a chemosensor for urea with a LOD of 45 μM. The underlying sensing principle is an instantaneous color change associated with the complex forming between the probe and ammonia, a hydrolysis product of urea catalyzed by the enzyme urease. In addition, the probe has a broad scope in sensing biologically significant amines such as arginine and lysine across a wide range of pH (4 to 8). Through extensive spectroscopic and computational studies in conjunction with control experiments, the importance of H-bonding in the sensing mechanism has been unraveled, revealing the stoichiometry, binding constant and LOD of these analytes with the probe. Indeed, the two individual amino acids can be distinguished by the spectral changes associated with UV-vis spectroscopy or by contrasting color diffusion under agarose gel conditions. Moreover, the probe shows a broad scope in detecting a range of aliphatic primary and secondary amines, including cyclic amines. The utility of the probe has also been demonstrated by using it for sensing urea in urine samples. These attributes make this probe a cost-effective, reusable and versatile chemosensor with ease of handling for sensing multianalytes by varying the conditions and detection modes.

1. Introduction

Urea is a crucial molecule in several biomolecular processes with distinct roles, such as a fertilizer for plants, a chief metabolite of nitrogen-rich biomolecules and an important molecular agent for the denaturation of proteins.[1–3] Despite being known for its low ecotoxicity, long-term exposure to excessive levels of urea causes soil acidification, eutrophication, groundwater pollution, ammonia emissions, *etc*.[4] In humans, urea is exclusively synthesized in the liver, transported through the bloodstream and excreted through body fluids like urine, sweat, serum, *etc*.; therefore, urea is one of the biomarkers for liver and kidney function, and is routinely quantified in clinical laboratories.[5,6] Thus, the qualitative and quantitative determination of urea is essential in a wide range of fields, including clinical diagnostics, environmental monitoring, agriculture and food science.[1,2,5,6] In this regard, several colorimetric, degradation-based, potentiometric, fluorometric and chemiluminescence-based assays of urea
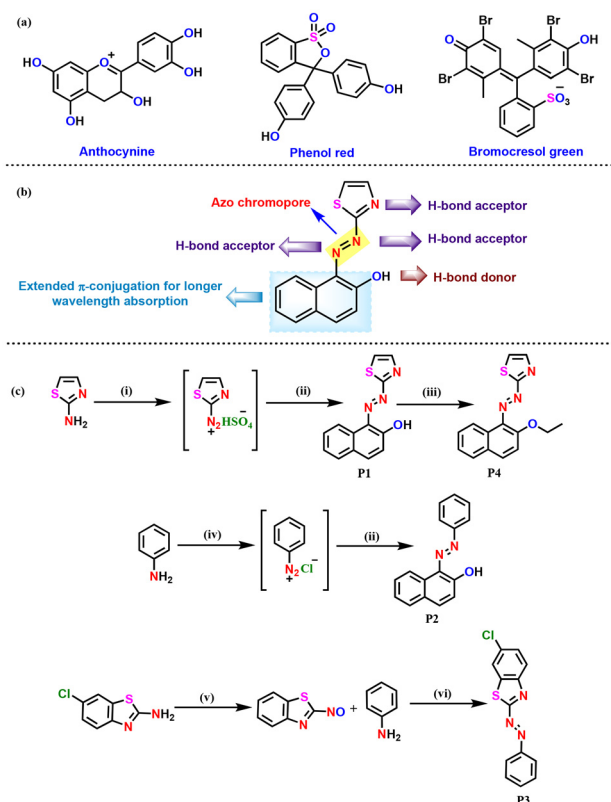
have been reported.[7–12] Alternatively, the methods of enzymatic degradation of urea followed by colorimetric and fluorometric assays are more viable.[13] Among them, the use of nickel-based urease enzyme for the selective and fast hydrolysis of urea to produce ammonia (NH_3) and carbon dioxide (CO_2) followed by sensing with acid–base or redox indicators is quite significant (Scheme 1a).[14,15] Given the increasing importance and demand for efficient urea detection, developing cost-effective colorimetric and fluorometric probes that are operationally simple, do not require sophisticated instrumentation and are compatible with neutral aqueous conditions is necessary for sensing real-life samples.[16–18]

In this regard, we envisioned an azo compound with appropriate substituents and complementary binding sites as a colorimetric probe having three H-bond donor and one H-bond acceptor sites, which can change its color on binding with ammonia. Our hypothesis relies on the response of the strong absorption properties of the azo chromophore upon analyte binding (Scheme 1b).[19,20] In addition, the *trans–cis* photoisomerization and the inherent thermal relaxation of the *cis* isomer could be an additional handle for improving the detection limit and spatiotemporal control in sensing.[21–25] Conversely, substitution-induced hindrance to photoswitching in certain azo systems can induce a fluorescence response that can enhance the detection limit.[26,27] In this context, we

Department of Chemical Sciences, Indian Institute of Science Education and Research (IISER) Mohali, Sector 81, SAS Nagar, Knowledge City, Manauli – 140 306, Punjab, India. E-mail: smaiti@iisermohali.ac.in, sugumarv@iisermohali.ac.in
†Electronic supplementary information (ESI) available. See DOI: https://doi.org/10.1039/d5ob00077g

3634 | *Org. Biomol. Chem.*, 2025, **23**, 3634–3642

This journal is © The Royal Society of Chemistry 2025

Scheme 1 (a) Representative chemosensors for urea detection; (b) design and key features of probe **P1** and (c) synthesis of the target and control probes: (i) NaNO$_2$, H$_2$SO$_4$, H$_2$O, 0–5 °C; (ii) 2-naphthol, NaOH, EtOH–H$_2$O, 0–5 °C to rt, 70%; (iii) K$_2$CO$_3$, EtI, DMF, 60 °C, 6 h, 75%; (iv) NaNO$_2$, HCl, H$_2$O, 0–5 °C, 90%; (v) Oxone®, H$_2$O, MeOH : CHCl$_3$ (1 : 5), reflux, 12 h, 40%; and (vi) AcOH, rt, 12 h, 55%.

designed an azothiazole probe comprising H-bonding acceptor sites and a β-naphthol unit, having a potential H-bond donor (OH group). As a proof-of-concept, the designed probe was tested by adding aqueous ammonia, resulting in a contrasting color change indicative of complexation. In addition, the probe showed versatility in binding with selective amino acids (arginine and lysine) and certain primary and secondary aliphatic amines. In particular, understanding the biological significance of arginine and lysine paves the way for their sensing and quantification, which is quite critical in viral infections and in the diagnosis of rare metabolic disorders like cystinuria and hyperlysinemia, respectively.[28,29] Although these two amino acids can be detected in various ways, developing cost-effective, rapid, sensitive and selective sensors has high potential.[30–36]

Herein, we report a molecular probe with a broad scope for sensing multiple analytes of biological importance, especially urea, arginine and lysine. Extensive spectroscopic and computational studies and control experiments unraveled their binding and sensing mechanisms. More importantly, the probe's real-life applications as a multi-analyte chemosensor was demonstrated using urine samples, highlighting its broad scope in detection.

## 2. Results and discussion

2.1. Design and synthesis

The target azothiazole-based probe **P1** for sensing ammonia (in turn, urea) was synthesized, as shown in Scheme 1c. The location of the hydroxy functionality *ortho* to the azo group facilitates tautomeric equilibrium between the azo (*enol* form) and hydrazone (*keto* form) forms *via* intramolecular proton transfer.[26,37–39] To understand the binding modes with the analyte and to establish the sensing mechanism, three additional probes (**P2–4**) were also synthesized (Scheme 1c).

2.2. Colorimetric studies

The preliminary testing was performed by inspecting the color changes before and after adding 10. eq. of aqueous ammonia solution (20%) to probe **P1** in DMSO (50 μM). The orange colored probe instantaneously turned pink upon the addition of ammonia (Fig. 1a). Following this, experiments were performed with a solution of urea (200 μM in Milli-Q water) and the probe (50 μM in DMSO) in a water–DMSO (8 : 2) mixture by adding the urease enzyme (20 nM in Milli-Q water). No color change was observed when a mixture of urea and the probe or urease and the probe was incubated, even for extended periods. However, the color changed from orange to pink within five to ten minutes when all three components were present, confirming the formation of ammonia and its complexation with the probe (Fig. 1b and movie M1 in the ESI†). Afterwards, the probe was also screened with various amino acids. In this regard, to a solution of probe **P1** (50 μM in DMSO), different aqueous amino acid solutions (10 eq. each) were added. Except for arginine and lysine, no other amino acid responded with a color change, demonstrating the utility of the probe for the detection of urea and selective amino acids by the naked eye (Fig. 1c).

2.3. Spectroscopic and computational studies

Next, experiments were performed and analyzed using UV-vis spectroscopy for quantitative detection. This study also hinted at the absence of photoisomerization of probe **P1**, irrespective of the irradiation wavelength (see section S2.1 in the ESI†).
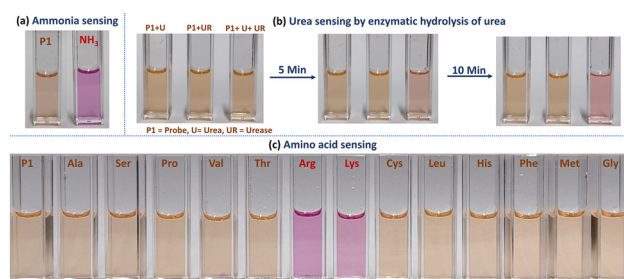
Fig. 1 Photographic images depicting solution phase naked-eye (a) detection of aqueous ammonia; (b) sensing of ammonia released during enzymatic hydrolysis of urea by urease; and (c) selective detection of arginine and lysine among various amino acids through color change of probe **P1**.

This journal is © The Royal Society of Chemistry 2025

Org. Biomol. Chem., 2025, **23**, 3634–3642 | **3635**

This can be attributed to the tautomerization through hydrogen bonding between hydroxyl and the azo functionalities and the consequent fast thermal relaxations.[26,37,39] Due to challenges in maintaining the concentration of ammonia and also the need for enzymatic conditions for probing urea, the majority of the optimizations were done using arginine (Arg) and lysine (Lys) as analytes. Firstly, UV-vis spectroscopic studies were carried out using various solvents, including CH_3CN, MeOH, EtOH, dioxane, DMSO, DMF and THF, in combination with H_2O to assess the impact of the solvent on the probe's binding and sensing capabilities. Except for DMSO and DMF, no other solvent mixture with water showed the ability for sensing of arginine and lysine (see Fig. S2.5 in the ESI†). In a DMSO–H_2O mixture (2 : 8 v/v), probe **P1** showed an absorption band centered at 490 nm without targeted analytes. When Arg or Lys was introduced into the solution, a significant bathochromic shift of 60 and 16 nm was observed (Fig. 2a). On titrating probe **P1** against Arg, a progressive increase in the band intensity centered around 545 nm was observed, indicating more complexation. Similarly, a band centered around 506 nm was observed with incremental addition of Lys solution to the probe (see Fig. S2.6 in the ESI†). The distinct shifts in the emerging bands relative to the absorption
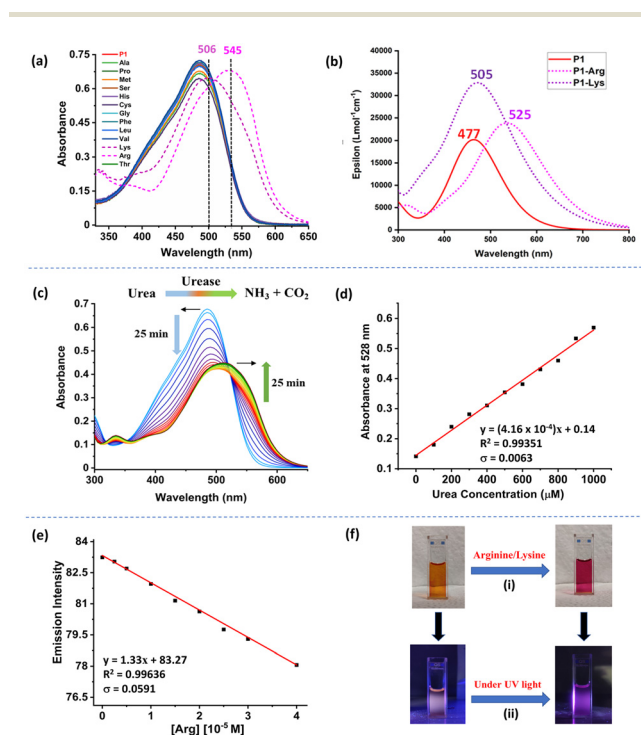
band of probe **P1** can distinguish the individual amino acids, arginine and lysine. All these results corroborated well with the computational data (Fig. 2b and see section S7 in the ESI†).

Considering the maximum intensity change in the absorption profile at 560 nm, we made a linear calibration plot between the analyte (arginine) concentration (5 to 40 μM) and the absorbance at 560 nm. From the linear calibration plot and using the formula $3\sigma/m$ (m, slope of the linear plot and σ, the standard deviation), the limit of detection (LOD) for arginine was estimated to be 0.9 μM (see Fig. S3.1a in the ESI†). Similarly, the LOD for lysine under identical conditions (at 560 nm, the non-overlapping shoulder absorption) was found to be 1.79 μM (see Fig. S3.2a in the ESI†). These results indicated the reasonably higher sensitivity of **P1** towards arginine than towards lysine. Association (or binding) constants (K_a) for both the analytes with the probe were estimated using Benesi–Hildebrand (B–H) plots. The slope of the linear fit revealed the binding constants to be $(1.41 \pm 0.06) \times 10^4$ M^{-1} and $(3.64 \pm 0.03) \times 10^4$ M^{-1} for arginine and lysine, respectively (see sections S3.1b and S3.2b in the ESI†). Furthermore, the stoichiometric ratios between the probe and the amino acids were estimated using Job's plot. The absorption changes at 560 nm of different mole fractions of probe **P1** and the individual amino acids were examined in this regard. The resulting Job's plot revealed a 1 : 1 complexation between the probe and arginine, whereas lysine showed a stoichiometry of 2 : 1 (**P1** : Lys) (see sections S3.1c and S3.2c in the ESI†). Similar titration experiments were also adopted for urea sensing with the help of the urease enzyme (5, 10, and 20 nM). The kinetics mode experiments and UV-vis spectroscopic analysis revealed that a minimum of 10 minutes is required for maximum absorption changes (Fig. 2c). Accordingly, screening experiments were performed with an incubation period of 10 minutes at various urea concentrations ranging from 100 μM–10 mM (see Fig. S3.3 in the ESI†). Following these data, the LOD has been estimated to be 45 μM using a linear calibration up to 1 mM (Fig. 2d).

Since probe **P1** was not exhibiting photoisomerization, we examined its fluorescence behavior in the DMSO/H_2O (2 : 8, v/v) mixture, where it showed moderate emission. A solution of **P1** showed broad fluorescence emission centered at 590 nm upon excitation at 490 nm. Interestingly, the addition of arginine (in incremental mode) led to the quenching of the emission intensity at 590 nm with the emergence of a bathochromic shifted emission signal centered at 620 nm (see Fig. S3.4 in the ESI†). The LOD was estimated to be 0.13 μM using a linear calibration from 5 to 40 μM arginine concentration (Fig. 2e). A similar behavior was also observed upon the addition of lysine to **P1**. Conversely, other amino acids showed no impact on the emission behavior of **P1** under similar conditions.

Fig. 2 (a) Absorption spectra of **P1** (40 μM) and the spectral changes in the amino acids (10 eq. in a DMSO−H_2O mixture); (b) TD-DFT computed UV-vis absorption spectra of **P1**, **P1**-Arg, and (**P1**)$_2$-Lys (in DMSO as a solvent using the PCM model); (c) scanning kinetics for absorption changes in **P1** (40 μM) during urea (500 μM) hydrolysis by urease (5 nM); (d) linear calibration plot of absorbance *vs.* concentration of urea; (e) linear calibration plot of emission intensity *vs.* concentration of arginine; and (f) images of the cuvette before and after addition of arginine (i) under normal light and (ii) under UV light.

2.4. Mechanism of sensing and control experiments

Next, we focused on the sensing mechanism and explored the reason for the preferential binding of arginine, lysine, and

3636 | *Org. Biomol. Chem.*, 2025, **23**, 3634–3642

This journal is © The Royal Society of Chemistry 2025

ammonia with **P1**. A pH-dependent complexation study was conducted to comprehend the impact of protonation and deprotonation on complexation. Firstly, the pH sensitivity was investigated by recording the absorption spectra of probe **P1** across a pH range from 3 to 11. The presence of a hydroxyl group made probe **P1** sensitive to basic pH conditions. As expected, a color change (orange to pink) was observed upon increasing the pH from 7 to 11. The UV-vis spectroscopic data accompanying this pH titration revealed a consistent batho-chromic shift towards a new band centered around 540 nm with a maximum absorbance at pH 11. This can be attributed to the deprotonation of the hydroxyl proton. Varying the pH between 7 and 5 resulted in no change in the spectrum or color of the solution; however, below pH = 4, a prominent blue shift in the azo π–π* band was observed that was accompanied by a color change from orange to yellow (see Fig. S4.1a and 1c in the ESI†).

Considering the presence of different H-bond acceptor sites such as azo nitrogen, thiazole nitrogen, and hydroxyl proton, the acidic pH could influence the protonation of any of these sites, leading to such observations (see Fig. S4.1d in the ESI†).

To understand the effect of pH on the **P1**–Arg complex, **P1** was dissolved in a phosphate buffer (10 mM) solution in the pH range of 3 to 11. Complex formation was observed in the pH range of 4 to 8, based on the expected spectral features around 540 nm. Similar experiments were performed for lysine. Lysine also showed rapid complex formation in the pH range of 4 to 8. Outside this pH range, protonation or deproto-nation of the probe/amino acid leads to blocking of binding sites and inhibition of complexation. These variable pH studies gave insights into the involvement of multiple probe sites in the complex formation (see Fig. S4.1b in the ESI†).
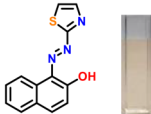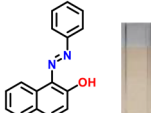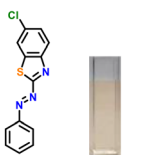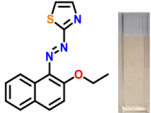
Considering the criticality of identifying the preferred binding sites in **P1** for the sensing mechanism, we screened three additional probes **P2–4** having structural variations. For control experiments, all probes were designed to remove or block potential binding sites selectively. In probe **P2**, the thia-zole unit of **P1** was replaced with a phenyl ring. On the other hand, probe **P3**, having a 6-chlorobenzothiazole unit, was syn-thesized. Additionally, a 2-naphthol unit was replaced with a phenyl ring in **P3**. In **P4**, the hydroxyl group was converted into –OEt through *O*-ethylation.

All the probes were tested independently with 10 eq. of lysine and arginine or ammonia; however, none of them exhibited color or spectral changes in response to Arg and Lys, but **P2** showed a color change in the presence of ammonia (Table 1). All the control experiments with the newly designed probes **P2–4** demonstrated the significance of cooperative binding in the sensing mechanism.

To identify the binding sites, titrations were carried out using ^{1}H NMR spectroscopy between probe **P1** and the analytes argi-nine and lysine. Prior to that, the proton signals of probe **P1** were unambiguously assigned using 2D NMR spectral data, including ^{1}H–^{1}H correlation spectroscopy (COSY), heteronuclear single quantum correlation (HSQC), and heteronuclear multiple bond correlation (HMBC) (see Fig. S4.2 in the ESI†).

Upon incremental addition of arginine from 0.5 eq. to 7.5 eq. in 5% D_2O in DMSO-d_6 into a solution of **P1** in DMSO-d_6 (5 mM), the proton signal at 8.45 ppm showed a downfield shift up to 8.87 ppm. In contrast, all other proton signals showed upfield shifts (Fig. 3a). These proton shifts arise from a strong interaction between arginine and the probe molecule. Also, the upfield shifts of the protons corroborate well with the changes in the computed Mulliken charges on the protons of

Table 1 Control experiments demonstrate the cooperative binding in **P1** and no detection with probes **P2–4**, which feature structural modifications for the selective sensing of arginine, lysine and ammonia

Structure	Probe	Arginine	Lysine	Ammonia	Detection
	P1	✓	✓	✓	
	P2	X	X	✓	
	P3	X	X	X	
	P4	X	X	X	
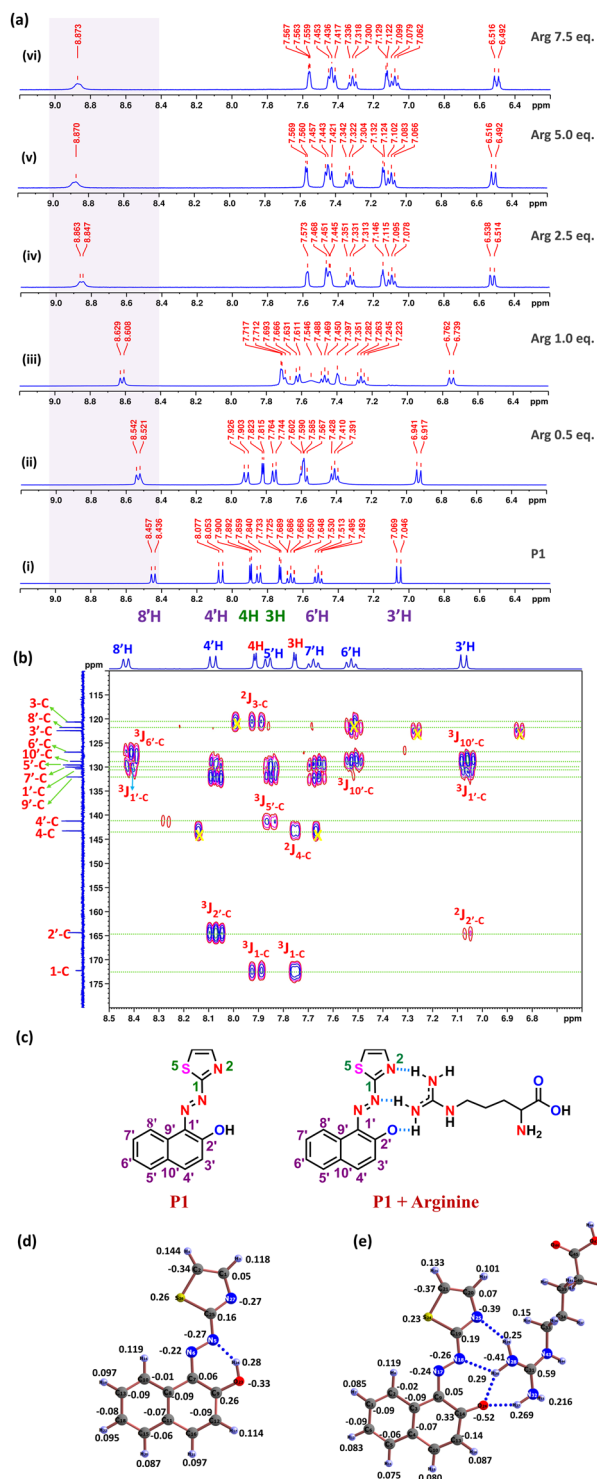
Fig. 3 (a) ^{1}H NMR titration of **P1** (5 mM) in DMSO-d_6 + D$_2$O, 9.5 : 0.5 v/v; (i) Probe **P1**; (ii) **P1** + 0.5 eq. arginine; (iii) **P1** + 1 eq. arginine; (iv) **P1** + 2.5 eq. arginine; (v) **P1** + 5 eq. arginine; (vi) **P1** + 7.5 eq. arginine. (b and c) Tentative assignments of probe **P1** based on 2D NMR (HMBC) analysis. Mulliken charges of **P1** (d) before and (e) after complexation with arginine (computed at the B3LYP-D3/6-311G(d,p) level of theory).

probe **P1** before and after complexation with arginine (Fig. 3d and e). Surprisingly, the Mulliken charge at 8′H of probe **P1** did not change upon complexation, indicating the possibility of weakening of the shielding effects due to azo nitrogen, leading to a higher chemical shift. Similar spectral changes were also observed for the complexation of the probe with ammonia and lysine; however, in the case of lysine, the shifts were limited, confirming the 2 : 1 complexation (see Fig. S4.3 and S4.4 in the ESI†). The spectroscopic and computational results on binding studies between the probe and the analytes (arginine, lysine and urea/NH$_3$) are summarised (Table 2).

2.5. Colorimetric detection with paper and in gel medium

To make this sensing procedure more practical, Whatman filter paper strips were dip-coated with a solution of **P1** in THF (500 μM), followed by air drying for 24 hours.[40] These paper strips were independently tested with 5 mM each of arginine and lysine solution. Similar to solution phase sensing, both amino acids induced color changes in the paper strips from orange to pink. Under identical experimental conditions, lysine showed a weaker color change due to the need for higher probe concentration to form the 1 : 2 complex. Conversely, the other amino acid failed to produce color changes. Similar color changes were also produced upon keeping the strip in close contact with ammonia fumes (Fig. 4a). Thus, the contrasting color change enables visual detection of ammonia formation during enzymatic urea hydrolysis using this paper strip test.

Additionally, the sensing studies were extended to gel-based techniques to examine their practical use.[41] Unlike conventional methods that involve laborious procedures and require expensive equipment or additional energy sources, gel media offer the advantages of easy handling, cost effectiveness, and a simple experimental protocol, while providing a clear colorimetric signal visible to the naked eye. Moreover, the diffusion of the analyte over a given time can be tracked by measuring the width of the contrasting-colored band, enabling both qualitative and quantitative sensing.[42,43] Probe **P1** (40 μM) was mixed with 0.5 wt% agarose powder in a DMSO : H$_2$O (2 : 8 v/v, 5 ml) mixture to form a gel. Afterwards, 30 μL aqueous solutions with varying equivalents of Arg and Lys (in the range of 5 eq. to 40 eq.) relative to the probe were added to different vials. Consequently, the diffusion of pink-colored bands was tracked over time. In contrast to solution phase detection, arginine exhibited a remarkable color change even at 5 equivalents, whereas lysine showed only a slight change at a higher equivalence (30–40 eq.) (Fig. S5.1 in the ESI†). The difference in stoichiometric ratios of both amino acids is attributed to this observed trend. A 1 : 1 complexation ratio with arginine allows efficient detection even in the condensed phase of the probe. In contrast, two probe molecules are necessary to bind with lysine, which is less probable in the gel form.

The gel-based sensing was further extended to urea sensing. Indeed, the pH tolerance and broad pH sensing range of probe **P1** make it an ideal candidate for monitoring the decomposition of urea under enzymatic hydrolysis.[44] Probe **P1**

3638 | *Org. Biomol. Chem.*, 2025, **23**, 3634–3642

This journal is © The Royal Society of Chemistry 2025

Table 2 Summary of binding studies between **P1** and arginine, lysine and urea

S. no.	Parameter	Method	Technique	Arginine	Lysine	Urea/NH$_3$
1	Stoichiometry	Job's plot (computational[a])	UV-vis	1 : 1	1 : 2	1 : 1[a]
2	Absorption band (λ_{max}/nm)	Titration	UV-vis	545	506	528
	Emission band ($\lambda_{ex}/\lambda_{em}$/nm)		Fluorescence	490/590	490/590	490/590
3	Association constant K_a (M^{-1})	Benesi–Hildebrand plot	UV-vis	1.41 × 10^4	3.64 × 10^4	—
4	Limit of detection, LOD (μM)	Linear calibration plot	UV-vis	0.91	1.79	45
			Fluorescence	0.13	—	—
5	Binding energies (kcal mol^{-1})	Computational[a]	Computational[a]	−9.4	−27.6	−32.5
6	Binding sites	Titration (computational[a])	NMR	N=N, OH, N thiazole of **P1**[b]		

[a] Computations were performed at the B3LYP-D3/6-311G(d,p) level of theory. [b] The backbone amine of the lysine/guanidine part of arginine or the NH$_2$ part of ammonia was predicted to be the complementary binding site of the analytes.
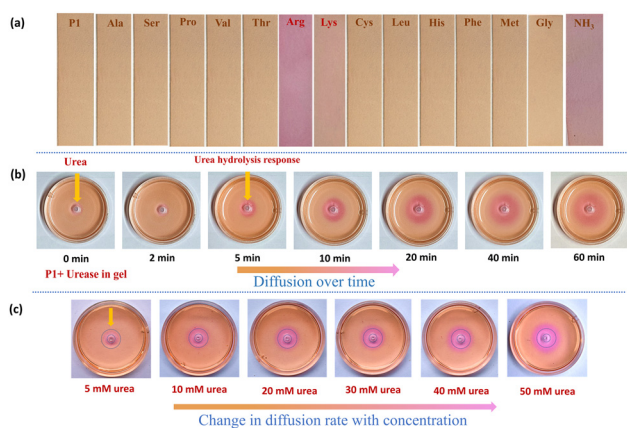
Fig. 4 Demonstration of visual detection of (a) amino acids (as 5 mM aqueous solution) and ammonia (as fumes) using **P1** dip-coated paper strips; (b) ammonia formation during diffusion of 60 mM urea (under enzymatic hydrolysis) over time; and (c) ammonia formation and change in the diffusion area as the urea concentration changes from 5 to 50 mM (after 60 minutes; agarose gel containing **P1** (40 μM) + urease (20 nM)).

and aqueous urease solution were mixed with agarose solution (20% DMSO in Milli-Q water) at 40 °C for these studies. After incubation for 5 minutes, this mixture was poured into a Petri dish for complete gelation. To a series of gels, 30 μL of each of the different solutions of urea (5 mM to 60 mM) was added at the center of each gel (for details, see the Experimental section). As urea diffuses in the gel medium, its reaction with urease produces ammonia as a product, leading to a visible pink colored band around the center. Over time, more diffusion of urea into gel caused the expansion of the pink hue (Fig. 4b). The diffusion rate of this pink zone can also be controlled by changing the urea concentration. As the urea concentration was increased, more diffusion of the pink band in the gel was observed (Fig. 4c and see Fig. S5.2 in the ESI†). Thus, the concentration-dependent diffusion of the band can be used to estimate urea in urine and soil samples.

2.6. Scope of detection

Besides urea/ammonia and amino acid (arginine and lysine) sensing, probe **P1** was also explored to sense other analytes. Given its selective binding with ammonia and the amino acid lysine, both of which have backbone primary amines, we were motivated to extend our study to various amines (Fig. 5a). Probe **P1** showed excellent selectivity towards primary and secondary aliphatic amines such as hexyl amine; however, it failed to detect tertiary amines under similar experimental conditions. Interestingly, secondary amines (diisopropyl amine) and cyclic amines (pyrazine and morpholine) also showed binding with the probe, inducing a color change from orange to pink. Further screening with aryl amines (aniline, benzylamine) was also performed with probe **P1**. Surprisingly, aniline showed no color or spectral changes upon addition to **P1**, even at higher equivalents, whereas benzylamine showed binding with a contrasting color change. Thus, the probe is versatile and can detect various aliphatic primary, secondary, and cyclic amines.

To evaluate the feasibility of **P1** for real-life applications, a commercially available urine sample was diluted 300 times with Milli-Q water before measurements. The bulk urine sample was then spiked with urea using a standard addition method and incubated with probe **P1** for 5 minutes in a 20% DMSO–H$_2$O mixture. Afterwards, 20 nM urease was added, and
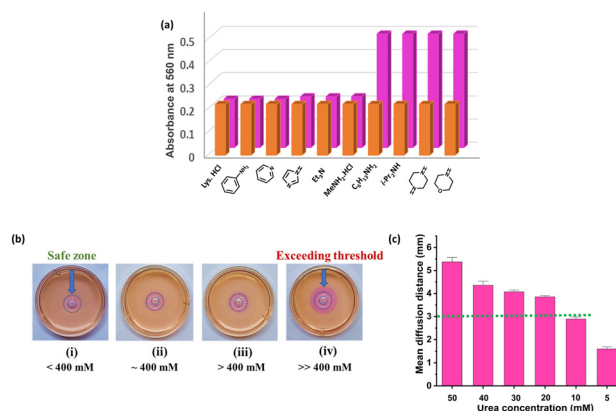
Fig. 5 (a) Histogram representing absorption change at 560 nm in the presence of various amines. (b) Picture depicting the diffusion of the detection zone upon varying the concentration of urea in urine samples (photographs were taken after 60 minutes; the safe zone is indicated with a blue-dotted circle). (c) Histogram depicting the mean diffusion distance (mm) relative to the urea concentration (mM) (the safe diffusion limit is indicated with a green dotted line).

This journal is © The Royal Society of Chemistry 2025

Org. Biomol. Chem., 2025, **23**, 3634–3642 | **3639**

the sample was again incubated for 10 minutes. The procedure was repeated 3–4 times with each sample and absorption changes at the 528 nm band were used to estimate urea in the urine sample (177.3 mM, 227.5 mM and 326.7 mM) (see Fig. S5.3 in the ESI†). Recovery experiments indicated excellent recovery efficiency (98.9–100.4%) of probe **P1** (see Table S5.1 in the ESI†). We also investigated urea detection in urine with agarose gel. A commercially available urine sample was spiked for the sensing experiment with different known urea concentrations. Next, these four samples were diluted 40 times with Milli-Q water and added to the centre of the agarose gel (Fig. 5b). The diffusion area was monitored visually for two hours. The diffusion area of 10 mM urea (calculated diffusion distance of 2.98 mm) was selected as a safe range for this experiment. After 60 minutes, we observed the diffusion range around the blue-dotted circle to analyze the urea concentration. In the first sample, only a light pink color was observed, indicating a very low concentration of urea (<400 mM). The second sample showed diffusion up to the safe zone (approximately 400 mM). In the third sample, a slightly higher diffusion was observed, which confirmed the excess urea above the threshold value. On the other hand, sample four exhibited high diffusion, indicating an abnormal level of urea in the urine sample (Fig. 5c, see Fig. S5.4 and Table S5.2 in the ESI†). Furthermore, probe **P1** was also tested for long-term stability and reproducibility. The probe showed consistent sensing of arginine in all detection media for several days. The spectral changes corresponding to complex (**P1 + Arg**) spontaneously returned to the initial absorption of **P1** upon the addition of phosphate salt (see section S6 in the ESI†).

3. Conclusions

In conclusion, we have developed an azothiazole-based probe for the qualitative and quantitative detection of ammonia, arginine and lysine through a spontaneous colorimetric color change from orange to pink in the solution phase and spectroscopic assays, respectively. The limit of detection from the absorption spectroscopic measurements was found to be 0.9 μM (UV-spectroscopy) for arginine 1.79 μM for lysine, and 45 μM for urea, which can be further extended as the probe showed fluorescence quenching during the complexation. A linear relationship of fluorescence quenching with increasing arginine concentration gave an improved LOD of 0.13 μM. The stoichiometric ratio and binding mechanism with both amino acids were studied extensively using experimental and computational methods. Coated paper strips and agarose-based hydrogel of probe **P1** enabled sensing of targeted analytes in the solid state. In the solid state, probe **P1** showed a better response towards ammonia and arginine than towards lysine due to the variation in the stoichiometry of the complexation. Quick detection of ammonia in solution and in the solid state provided the scope to monitor urea hydrolysis catalyzed by the urease enzyme. The contrasting color change and the rate of diffusion in the sensing zone allowed qualitative and quanti-

tative estimation of urea in urine samples without requiring expensive and sensitive instruments or complex procedures. In addition, the probes show color changes with selected aliphatic primary and secondary amines, including cyclic amines, besides the detection of arginine and lysine. Thus, the azothiazole-based probe has shown excellent utility as a multi-analyte chemosensor for biologically significant species in a simple and reusable manner. Despite the probe exhibiting non-selective detection, its broad sensing capability could be useful in the detection of several amino functional groups containing biologically active molecules, including markers for food spoilage and amine detection in solid-state peptide synthesis.[45–47]

4. Experimental section

4.1. Synthesis of targeted probes

4.1.1. Synthesis of (*E*)-1-(thiazol-2-yldiazenyl) naphthalen-2-ol (P1). To a suspension of 2-amino thiazole **1** (2 g, 20 mmol) in 10 ml H_2O at 0 °C, conc. H_2SO_4 (5 ml) was slowly added. The solution was stirred for 10–15 min. Then an aqueous solution of $NaNO_2$ (1.7 g, 25 mmol) was added dropwise to the prepared suspension at 0 °C. In a separate beaker, a mixture of 2-hydroxy naphthalene **2** (2.8 g, 20 mmol) and NaOH (1.6 g, 40 mmol) in ethanol (15 ml) was prepared. Both the solutions were stirred separately for 20 min. The diazonium salt solution of **1** was then added into the solution of **2** in a dropwise manner and stirred for half an hour.[37,38] A red coloured precipitate was formed, which was filtered off. This was purified by column chromatography using an ethyl acetate : *n*-hexane (5 : 95) mixture as an eluent to yield the desired product. Red solid, 70% yield, M.P. 150–152 °C, ^1H NMR (400 MHz, DMSO-d_6): δ 14.66 (s, 1H), 8.47 (d, *J* = 8.3 Hz, 1H), 8.12 (d, *J* = 9.3 Hz, 1H), 7.92 (d, *J* = 3.3 Hz, 1H), 7.89 (d, *J* = 7.9 Hz, 1H), 7.78 (d, *J* = 3.3 Hz, 1H), 7.70 (t, *J* = 7.5 Hz, 1H), 7.55 (t, *J* = 7.5 Hz, 1H), 7.10 (d, *J* = 9.3 Hz, 1H) ppm; ^{13}C NMR (100 MHz, DMSO-d_6): δ 171.8, 163.9, 142.8, 140.7, 131.6, 129.9, 129.5, 129.1, 128.3, 126.4, 122.0, 121.3, 120.1 ppm; FT-IR (ATR, cm^{-1}): 3080, 3072, 1615, 1483, 1405, 1298, 1234, 1184, 977; HRMS (ESI): *m/z* calcd for $C_{13}H_{10}N_3OS$ [M + H]$^+$: 256.0544, obs.: 256.0535

4.1.2 Synthesis of (*E*)-1-(phenyldiazenyl) naphthalen-2-ol (P2). To a mixture of aniline **3** (1 g, 10.8 mmol) in H_2O, conc. HCl (2.5 ml) was added dropwise at 0 °C. The solution was stirred for 10–15 min and then aq. $NaNO_2$ (0.86 g, 13.4 mmol) was added dropwise. In another beaker, a mixture of 2-hydroxy naphthalene **2** (1.5 g, 10.8 mmol) and NaOAc (3.5 g, 43.2 mmol) in ethanol (15 ml) was prepared. Both the solutions were stirred separately at 0 °C for 20–25 min. To the diazonium salt of **3**, the solution of 2-hydroxy naphthalene was added in a dropwise manner. A red coloured precipitate was formed, which was filtered off. This was purified by recrystallization in *n*-hexane. Red solid, 90% yield, M.P. 142–143 °C. ^1H NMR (400 MHz, DMSO-d_6): δ 14.86 (s, 1H), 8.56 (d, *J* = 8.0 Hz, 1H), 7.97 (d, *J* = 12.0 Hz, 1H), 7.88 (dd, *J* = 9.6, 8.4 Hz, 2H), 7.80 (d, *J* = 7.6 Hz, 1H), 7.65–7.60 (m, 1H), 7.58–7.54 (m, 2H),

3640 | *Org. Biomol. Chem.*, 2025, **23**, 3634–3642

This journal is © The Royal Society of Chemistry 2025

7.49–7.45 (m, 1H), 7.42–7.375 (m, 1H), 6.94 (d, J = 9.6 Hz, 1H) ppm; ^{13}C NMR (100 MHz, DMSO-d_6): δ (ppm) 168.9, 145.1, 140.0, 132.8, 129.8, 129.2, 129.1, 128.9, 128.1, 127.8, 125.9, 124.0, 121.3, 119.0; FT-IR (ATR, cm^{-1}): 3659, 3072, 2923, 1500, 1261, 1148, 842, 752; HRMS (ESI): m/z calcd for $C_{16}H_{13}N_2O$ [M + H]$^+$: 249.1028; obs.:249.1028.

4.1.3. Synthesis of 6-chloro-2-nitrosobenzothiazole (5). Compound **5** was synthesised using a procedure reported previously in the literature with few modifications.[48] A solution of Oxone® (11.85 g, 42.21 mmol) in 65 ml water was slowly added to a solution of 6-chloro-2-aminobenzothiazole **4** in 335 ml MeOH/CHCl$_3$ (1 : 5). The resulting mixture was refluxed for 12 h, and then cooled down to room temperature. The resulting solid precipitates were filtered off and the mother liquor was separated, dried over anhydrous Na$_2$SO$_4$, and evaporated under reduced pressure. The crude product **5** was purified by column chromatography using silica gel and n-hexane as an eluent and obtained as a green crystalline solid. This product **5** was used for the next step immediately without further characterization.

4.1.4. Synthesis of (E)-6-chloro-2-(phenyldiazenyl) benzo[d] thiazole (P3). Compound **5** (0.233 g, 1.18 mmol) was dissolved in AcOH (3 ml) and heated at 50 °C. This solution was then dropwise added into a solution of aniline **3** (0.109 g, 1.18 mmol) in AcOH (0.5 ml). The resultant mixture was stirred at room temperature overnight. A yellow-orange solid precipitated out, which was filtered off and washed with water (20 ml). After air drying, the precipitate was recrystallized from a diethyl ether/MeOH (2 : 8) mixture to yield the desired product as orange needles. Orange solid, 55% yield, M.P. 180–181 °C. ^{1}H NMR (400 MHz, CDCl$_3$): δ 7.93–7.86 (m, 3H), 7.82 (d, J = 2.0 Hz, 1H), 7.56–7.50 (m, 3H), 7.43 (dd, J = 8.5, 2.0 Hz, 1H) ppm; ^{13}C NMR (100 MHz, CDCl$_3$): δ 151.2, 146.4, 138.5, 132.6, 129.5, 128.9, 127.6, 126.8, 124.9, 123.2, 110.8 ppm; FT-IR (ATR, cm^{-1}): 3741, 2929, 2852, 1568, 1437, 1222, 1144, 1093, 824; HRMS (ESI): m/z calcd for $C_{13}H_9ClN_3S$ [M + H]$^+$: 274.0205; obs.: 274.0212.

4.1.5. Synthesis of (E)-2-((2-ethoxynaphthalen-1-yl) diazinyl) thiazole (P4). In a round bottom flask, **P1** (0.25 g, 0.88 mmol) and K$_2$CO$_3$ (0.36 g, 2.64 mmol) were suspended in 0.5 ml dry DMF. After stirring this mixture at 60 °C for 20 minutes, ethyl iodide (0.15 ml) was added and the reaction was continued at 60 °C for 12 hours. The reaction was monitored by TLC and after completion, the reaction mixture was quenched with water and extracted with ethyl acetate. The combined organic phase was dried over anhydrous Na$_2$SO$_4$ and evaporated under vacuum. The crude product was then purified by column chromatography using silica gel and ethyl acetate : n-hexane (2 : 98) mixture as an eluent. The product was obtained as a red liquid. Red liquid, 82% yield. ^{1}H NMR (400 MHz, CDCl$_3$): δ 8.96 (d, J = 8.7 Hz, 1H), 8.04 (d, J = 3.1 Hz, 1H), 7.96 (d, J = 9.0 Hz, 1H), 7.81 (d, J = 8.0 Hz, 1H), 7.63 (t, J = 7.4 Hz, 1H), 7.46 (t, J = 7.4 Hz, 1H), 7.41–7.34 (m, 2H), 4.36 (q, J = 7.0 Hz, 2H), 1.54 (o, J = 7.0 Hz, 3H,) ppm; ^{13}C NMR (100 MHz, CDCl$_3$): δ 179.7, 152.9, 143.8, 135.5, 133.8, 129.4, 129.2, 129.0, 128.2, 125.1, 124.4, 120.7, 115.7, 66.6, 15.1 ppm;

FT-IR (ATR, cm^{-1}): 2979, 2928, 1591, 1429, 1276, 1251, 1150, 808; HRMS (ESI): m/z calcd for $C_{15}H_{14}N_3OS$ [M + H]$^+$: 284.0857; obs.: 284.0851

Data availability

The data supporting this article have been included as part of the ESI.†

Conflicts of interest

There are no conflicts to declare.

Acknowledgements

References

1 G. Dhawan, G. Sumana and B. D. Malhotra, *Biochem. Eng. J.*, 2009, **44**, 42–52.

2 C. Zhuowei, L. Jingqiang, Y. Chunji, Y. Zaixing, W. Jianlan and Z. Ruhong, *J. Phys. Chem. B*, 2014, **118**, 48–57.

3 B. J. Bennion and V. Daggett, *Proc. Natl. Acad. Sci. U. S. A.*, 2003, **100**, 142–5147.

4 W. H. Hale, *J. Agric. Food Chem.*, 1956, **4**, 948–951.

5 J. Krämer, R. Kang, L. M. Grimm, L. D. Cola, P. Picchetti and F. Biedermann, *Chem. Rev.*, 2022, **122**, 3459–3636.

6 Y. Y. Broza, X. Zhou, M. Yuan, D. Qu, Y. Zheng, R. Vishinkin, M. Khatib, W. Wu and H. Haick, *Chem. Rev.*, 2019, **119**, 11761–11817.

7 X. Hu, Z. Ma, J. Li, Z. Cai, Y. Li, B. Zu and X. Dou, *Mater. Horiz.*, 2020, **7**, 3250–3257.

8 F. Wang, F. Zhang, Q. Wang and P. He, *Anal. Chem.*, 2022, **94**, 14434–14442.

9 R. Chaudhari, A. Joshi and R. Srivastava, *Sci. Rep.*, 2017, **7**, 5840.

10 Y. Cheng, X. Yi-Tong, H. Yu-Ting, Z. Hong, W. J. Xing-, L. Peng, C. Z. Yuan, Z. Ling, L. Peng, C. Guangxu and W. Z. Wei, *ACS Sens.*, 2023, **8**, 1835–1840.

11 A. M. Adane and S.-Y. Park, *ACS Sens.*, 2023, **8**, 2290–2297.

12 C. Celik, N. Y. Demir and M. Duman, *Sci. Rep.*, 2023, **13**, 2056.

13 L. Mazzei, M. Cianci, S. Benini and S. Ciurli, *Angew. Chem., Int. Ed.*, 2019, **58**, 7415–7419.

This journal is © The Royal Society of Chemistry 2025

Org. Biomol. Chem., 2025, **23**, 3634–3642 | 3641

14 Y. Chang, T.-E. Park, S.-W. Lee and E.-H. Lee, *Biosensors*, 2022, **12**, 886.

15 R. E. Mohamed, M. S. Samy, Y. E. Ahmed, H. Eslam, S. Jihoon, Y. C. Soo and H. K. Dong, *ACS Appl. Nano Mater.*, 2023, **6**, 7992–8003.

16 N. Y. Edwards, T. W. Sager, J. T. McDeviit and E. V. Anslyn, *J. Am. Chem. Soc.*, 2007, **129**, 13575–13583.

17 J. Chen, R. J. Hooley and W. Zhong, *Bioconjugate Chem.*, 2022, **33**, 2245–2253.

18 L. You, D. Zha and E. V. Anslyn, *Chem. Rev.*, 2015, **115**, 7840–7892.

19 Z. Jin, W. Yim, M. Retout, E. Housel, W. Zhong, J. Zhou, M. S. Strano and J. V. Jokerst, *Chem. Soc. Rev.*, 2024, **53**, 7681–7741.

20 M. S. Hossain, S. A. Rahaman, J. Hatai, M. Saha and S. Bandyopadhyay, *Chem. Commun.*, 2020, **56**, 4172–4175.

21 A. Srivastava, S. Grewal, S. Singh, Rajani and S. Venkataramani, *ChemPhotoChem*, 2023, **7**, e202300029.

22 A. Raman, G. Augustine, N. Ayyadurai and S. Easwaramoorthi, *J. Mater. Chem. C*, 2018, **6**, 10497–10501.

23 L. Stricker, E.-V. Fritz, M. Peterlechner, N. L. Doltsinis and B. J. Ravoo, *J. Am. Chem. Soc.*, 2016, **138**, 4547–4554.

24 A. Rananaware, M. Samanta, R. Bhosale, M. A. Kobaisi, B. Roy, V. Bheemireddy, S. V. Bhosale, S. Bandyopadhyay and S. V. Bhosale, *Sci. Rep.*, 2016, **6**, 22928.

25 F. Höglsperger, F. A. Larik, C. Bai, M. D. Seyfried, C. Daniliuc, H. Klaasen, P. Thordarson, J. E. Beves and B. J. Ravoo, *Chem. – Eur. J.*, 2023, **29**, e202302069.

26 H. M. D. Bandara and S. C. Burdette, *Chem. Soc. Rev.*, 2012, **41**, 1809–1825.

27 A. Chevalier, P.-Y. Renard and A. Romieu, *Org. Lett.*, 2014, **16**, 3946–3949.

28 F. Shiraseb, O. Asbaghi, R. Bagheri, A. Wong, A. Figueroa and K. Mirzaei, *Adv. Nutr.*, 2022, **13**, 1226–1242.

29 Z. Schmidt, G. Murthy, M. Ennis, S. S. Ipsiroglu and R. J. Elango, *Inherited Metab. Dis.*, 2020, **43**, 952–959.

30 X. Zeng, S. Wei, J. Hu, L. Gou, L. Wu and X. Hou, *Anal. Chem.*, 2022, **94**, 10271–10277.

31 X. Zhou, X. Jin, D. Li and X. Wu, *Chem. Commun.*, 2011, **47**, 3921–3923.

32 M. Fokkens, T. Schrader and F.-G. Klärner, *J. Am. Chem. Soc.*, 2005, **127**, 14415–14421.

33 L. Yang, Y. Xie, Q. Chen, J. Zhang, L. Li and H. Sun, *ACS Appl. Bio Mater.*, 2021, **4**(8), 6558–6564.

34 A. Chetry, J. Borah, U. N. Hazarika, D. J. Sonowal, S. Konwer and P. Khakhlary, *Anal. Methods*, 2024, **16**, 7390–7396.

35 A. Buryak and K. Severin, *J. Am. Chem. Soc.*, 2005, **127**, 3700–3701.

36 B. Lee, R. Scopelliti and K. Severin, *Chem. Commun.*, 2011, **47**, 9639–9641.

37 S. Devi, M. Saraswat, S. Grewal and S. Venkataramani, *J. Org. Chem.*, 2018, **83**, 4307–4322.

38 P. Kumar, A. Srivastava, C. Sah, S. Devi and S. Vekataramani, *Chem. – Eur. J.*, 2019, **25**, 11924–11932.

39 C. Sah, A. Mahadevan, P. Kumar and S. Venkataramani, *Phys. Chem. Chem. Phys.*, 2022, **24**, 7848–7855.

40 P. K. Chaturvedi and U. Maitra, *Sens. Diagn.*, 2024, **3**, 809–816.

41 Y. Wei, J. Tang, J. Zhang, Y. Lin and C. Zheng, *Chem. Commun.*, 2025, **61**, 1215–1218.

42 A. Q. Mai, T. Bánsági, A. F. Taylor and Sr. J. A. Pojman, *Commun. Chem.*, 2021, **4**, 101.

43 R. R. Mahato, Priyanka, E. Shandilya and S. Maiti, *Chem. Sci.*, 2022, **13**, 8557–8566.

44 E. Shandilya, A. S. Bains and S. Maiti, *J. Phys. Chem. B*, 2023, **127**, 10508–10517.

45 Y. J. Diaz, Z. A. Page, A. S. Knight, N. J. Treat, J. R. Hemmer, C. J. Hawker and J. R. de Alaniz, *Chem. – Eur. J.*, 2017, **23**, 3562–3566.

46 H. Li, J. Gan, Q. Yang, L. Fu and Y. Wang, *Talanta*, 2021, **234**, 122706.

47 T. Umeno, M. Fujihara, S. Matsumoto, N. Iizuka, K. Usui and S. Karasawa, *Anal. Chem.*, 2023, **95**, 15803–15809.

48 H. Faustino, C. R. Brannigan, L. V. Reis, P. F. Santos and P. Almeida, *Dyes Pigm.*, 2009, **83**, 88–94.